

CFD MODELLING OF FLOATING AND SETTLING PHASES IN SETTLING TANKS

K. MOHANARANGAM AND D. W. STEPHENS*

Parker Centre (CSIRO Minerals), Clayton, Victoria 3169, AUSTRALIA

*Darrin.Stephens@csiro.au

ABSTRACT

A Computational Fluid Dynamics (CFD) model for modelling a floating phase has been developed and tested on a settling tank. The current model used for settling tanks is able to predict the settling of solids and the formation of a higher density layer of solids at the bottom of the vessel. Due to the widespread use of settling tanks in water and other chemical industries, floating phases (cenospheres, oil, PVC, etc) form a major part of the separation process. With this in mind, a model has been developed to incorporate both the settling as well as the floating of the secondary phases. The simulations were performed by customizing the commercially available software ANSYS-CFX (release 10.0). Multi-phase simulations were performed with clay, sand and a floating solid (density less than the continuous phase) as the secondary phases. Numerical instability was encountered in the volume fraction of the floating phase at the top boundary, where the floating phase collected, when using the unmodified version of ANSYS-CFX. This was mainly due to the volume fraction tending towards unity without any gradient at the top boundary. To prevent this happening, an extra term that is ignored in the CFX implementation was included in the slip velocity calculation. This essentially sets up a volume fraction gradient of the floating phase. Two variants of particle sizes for the floating phase were used to access this phenomenon. Contour plots of the floating phase volume fraction are presented within the feedwell as well in the cross-section of the tank to depict the preferential concentration of the phase. Further results are also shown for the settling solids.

NOMENCLATURE

C_D	drag co-efficient
C_μ	k - ϵ turbulence model constant
$C_{\epsilon 1-2}$	k - ϵ turbulence model constant
d	diameter
g	acceleration due to gravity
k	Turbulence Kinetic Energy (T.K.E)
p	pressure
r	solids fraction
Re	Reynolds number
Sc_t	Turbulent Schmidt number
$S1-S2$	Diameter of floating species
t	time
U	velocity
Y	mass fraction
x,y,z	cartesian co-ordinate system
ϵ	turbulence dissipation rate
μ	dynamic viscosity

μ_{eff}	effective viscosity
μ_t	turbulent viscosity
σ_k	k - ϵ turbulence model constant
σ_ϵ	k - ϵ turbulence model constant
ρ	density
τ	viscous stress

Subscripts

m	mixture
D	diffusion
α	phase
$S\alpha$	phase slip velocity
$D\alpha$	phase drift velocity
p	particle
c	continuous phase

Superscript

i, j, k	cartesian velocity components
-----------	-------------------------------

INTRODUCTION

Secondary Settling Tanks (SST's) form a crucial component in gravity separation processes mainly in solid-liquid separation. They perform the crucial process of separating the activated sludge from the clarified effluent and also to concentrate the settled sludge. Many processes depend crucially on the performance of SST's, particularly in water and wastewater treatment facilities, where they can account for 30% of total plant investment (Brennan, 2001), and non-ideal hydraulics in settlers can be detrimental to solids removal performance (Vanrolleghem et al., 2006). Despite the practical importance of these tanks, current design practice relies heavily on empirical formulae which do not take full account of the detailed hydrodynamics of the system (Brennan, 2001). The determination of the removal efficiency for sedimentation tanks has been the subject of numerous theoretical and experimental studies. The removal efficiency depends on the physical characteristics of the suspended solids (e.g. particle size, density, and settling velocity) as well as on the flow field and the mixing regime in the tank.

A floating phase is a widespread issue in many industries. In addition to water and wastewater treatment facilities, they are found in many coal-fired power plants in ash clarifiers, wherein cenospheres/plerospheres form a low density material to be skimmed off from the top and used as fillers in many other applications. Floating phases are also encountered in many chemical industries where a suspension of particles is added to a liquid to promote a

chemical reaction between the phases, enhancing dissolution or creating some new product (Kuzmanic & Rusic, 1999). A floating phase is also observed in settling tanks within the Canadian oil sands industry, where residual bitumen complicates the recovery of hot wash water from tailings slurries (Moore, 2009).

A variety of techniques have been used to study and resolve the flow field characteristics found in settling tanks. Measurements using drogues were conducted by Anderson, (1945), Bretscher et al. (1992) and Ueberl and Hager (1997), while ultrasonic flow meters were used by Larsen (1977) and Fulford (1995). Krebs et al. (1998) evaluated electromagnetic velocity meters against Laser Doppler Velocimetry (LDV) in a lab-scale settling tank and found that the former were more accurate. Lyn and Rodi (1990) were able to characterize the mean velocity and the flow turbulence in the inlet region of a rectangular laboratory settling basin by means of a two-component Laser Doppler Anemometry (LDA) system. Recently, Vanrolleghem et al. (2006) have used a non-invasive ADCP (Acoustic Doppler Current Profiler) to characterize hydrodynamics in a secondary settler.

While physical measurements are the best way to fully understand the behaviour of liquor and solid flows, they cannot be ascertained before the tank is really built. Computational Fluid Dynamics (CFD) on the other hand offers an alternative way to give the design engineers predictions about this behaviour (Dufresne et al., 2009). Zhou and McCorquodale (1993) stated that the two important hydrodynamic factors affecting the solids distribution in secondary settling tanks are the strength of the bottom density current and the upward current near the effluent weirs, both of which can be predicted from CFD.

Numerical studies have been and are still being carried out in a range of settling tanks/clarifiers used within waste and water treatment facilities. These models have been progressively improved since Larsen (1977). Some of the numerical studies include Imam et al. (1983), Celik et al. (1985), Stamou et al. (1989), Adams and Rodi (1990), Stamou (1991), Lyn et al. (1992), Frost et al. (1993), Dahl et al. (1994), Johnston et al. (1996), Lakehal et al. (1999), Brennan (2001), Kahane et al. (2002), Adamsson et al. (2003), Jayanthi and Narayanan (2004), Nguyen et al. (2006), Fan et al. (2007), and Dufresne et al. (2009).

All the above numerical studies dealt with solids settling at the bottom of the tank and the clear liquor escaping at the top through the overflow. Studies concerning the draw-down of solids at the top through floatation have also been widely published. This mainly occurs due to the density difference between the liquid and the dispersed solids, poor wettability or low apparent bulk density, as detailed by Etchells (2001). The effect of impeller speeds and design in the draw-down of solids have been studied numerically (Taskin and Wei, 2003; Tagawa et al., 2006; Mackiewicz and Karcz, 2009; Khazam and Kresta, 2009). There have been comparatively few numerical studies combining both the floating as well as the settling solids as one whole system. This forms the main focus of the current paper, wherein numerical studies have been carried out on the effect of both the settling as well as the floating phases in a settling tank.

MODEL DESCRIPTION

Algebraic Slip Model

In Eulerian-Eulerian multiphase flow, the full momentum equation is considered, including inertial effects, wherein each phase has its own velocity field, governed by conservation of momentum for the phase. In some cases, however, if the time-scales to reach the equilibrium slip velocity are small, it is appropriate to use simplified models like the Algebraic Slip Model (ASM) for multiphase flow.

The ASM assumes the existence of one continuous medium/mixture with various dispersed phase components (particles, droplets, etc). This mixture behaves as a single fluid whose density and viscosity can be locally affected by the disperse components, and any number of ASM disperse components can be defined. In ANSYS-CFX each dispersed component is represented by a mass-fraction equation and relative movement is allowed between these components and the continuous phase (phase slip). The name of the model arises from the assumption that this phase slip can be modelled using a simple algebraic formula.

Governing Equations

The ASM model treats both the continuous as well as the dispersed phase as a single mixture with a slip (velocity) between them. The bulk continuity equation obtained by summing over all phases is given by equation (1).

$$\nabla \cdot (\rho U_m) = 0 \quad (1)$$

$$\frac{\partial (\rho_m u_m^j u_m^i)}{\partial x^j} = -\frac{\partial p}{\partial x^i} + \frac{\partial (\tau_m^{ji} + \tau_D^{ji})}{\partial x^j} + \rho_m g^i \quad (2)$$

The bulk momentum equation is given by equation (2); unlike an Eulerian two-fluid model there is no need for separate momentum equations for the dispersed phase(s). The mixture properties are given by

$$\rho_m = \sum_{\alpha} r_{\alpha} \rho_{\alpha} \quad (3)$$

$$\rho_m u_m^i = \sum_{\alpha} r_{\alpha} \rho_{\alpha} u_{\alpha}^i \quad (4)$$

$$\tau_m = \sum_{\alpha} r_{\alpha} \tau_{\alpha} \quad (5)$$

$$\tau_D^{ji} = -\sum_{\alpha} r_{\alpha} \rho_{\alpha} (u_{\alpha}^i - u_m^i) u_{\alpha}^j \quad (6)$$

Drift and Slip Relations

The slip velocity is given as the difference of the dispersed and the continuous phase velocities equation (7). The relation between the drift and the mixture is given by equation (8)

$$u_{S\alpha}^i = u_{\alpha}^i - u_c^i \quad (7)$$

$$u_{D\alpha}^i = u_{S\alpha}^i - u_m^i \quad (8)$$

$$u_{D\alpha}^i = u_{S\alpha}^i - \sum_{\alpha} Y_{\alpha} u_{S\alpha}^i \quad (9)$$

Based on the above formulation, the dispersed phase continuity equation is given by

$$\frac{\partial \rho_m Y_{\alpha}}{\partial t} + \frac{\partial}{\partial x^j} (\rho_m Y_{\alpha} (u_m^j + u_{D\alpha}^j)) = \rho_{\alpha} Y_{\alpha}'' u_m^{j''} \quad (10)$$

Slip Equation

The ASM comes with the following assumptions for the estimation of the slip velocity:

- i. Disperse phase is assumed to instantaneously reach its terminal velocity, so the transient term on the drift velocity is neglected. $\left(\frac{\partial u_{D\alpha}^i}{\partial t} = 0\right)$
- ii. The approximation is made that: $u_{\alpha}^i \frac{\partial \alpha^i}{\partial x^j} \approx u_m^i \frac{\partial \alpha^i}{\partial x^j}$
- iii. Viscous and apparent diffusion stresses are neglected in standard formulation of ANSYS CFX 10.0.

On further derivation along with the assumptions stated above, the slip velocity leads to a form given by equation (11)

$$|u_{s\alpha}^i| u_{s\alpha}^i = -\frac{4}{3} \frac{d_p}{\rho_c C_D} (\rho_{\alpha} - \rho_m) \left(\frac{\partial u_m^i}{\partial t} + u_m^i \frac{\partial u_m^i}{\partial x^j} - g^i \right) \quad (11)$$

where C_D is the drag coefficient. Various models of C_D are available based on the particle Reynolds number Re_p . At low particle Reynolds numbers (viscous regime) the drag coefficient is given by Stoke's law

$$C_D = \frac{24}{Re_p}, \quad Re_p \ll 1 \quad (12)$$

For large particle Reynolds number (inertial regime) the drag coefficient becomes independent of the Reynolds number and is given by

$$C_D = 0.44, \quad 1000 \leq Re_p \leq 1-2 \times 10^5 \quad (13)$$

In the transitional region between the viscous and inertial regimes, both viscous and inertial effects are important. Several empirical correlations are available for the drag coefficient in this regime. The one available in ANSYS-CFX is due to Schiller and Naumann (1933) and can be written as

$$C_D = \frac{24}{Re} (1 + 0.15 Re^{0.687}), \quad Re_p \leq 1000 \quad (14)$$

Turbulence Modelling

Reynolds Averaged Navier Stokes (RANS) equations based on eddy viscosity hypothesis are employed in this study for turbulence modelling. A two-equation $k-\epsilon$ model is used as the turbulent closure. The eddy viscosity of the resulting model is given by

$$\mu_t = C_{\mu} \rho_m \frac{k_m^2}{\epsilon_m} \quad (15)$$

where k_m and ϵ_m are solved as two separate transport equations given by equation (16) and (17), respectively.

$$\nabla \cdot (\rho_m u_m^j k_m) = \nabla \cdot \left[\left(\mu + \frac{\mu_t}{\sigma_k} \right) \nabla k_m \right] + P_k - \rho \epsilon_m \quad (16)$$

$$\nabla \cdot (\rho_m u_m^j \epsilon_m) = \nabla \cdot \left[\left(\mu + \frac{\mu_t}{\sigma_{\epsilon}} \right) \nabla \epsilon_m \right] + \frac{\epsilon_m}{k_m} (C_{\epsilon 1} P_k - C_{\epsilon 2} \rho_m \epsilon_m) \quad (17)$$

where C_{μ} , $C_{\epsilon 1}$, $C_{\epsilon 2}$, σ_k and σ_{ϵ} are constants.

In the ASM, the turbulent dispersion forces are not considered in the derivation of the slip velocity. Instead, turbulent dispersion is modelled using the eddy dissipation assumption in the transport equation for phase mass

fraction. This results in the following term being added to equation (10).

$$\overline{\rho_{\alpha} Y_{\alpha}'' u_m^{i''}} = \frac{\mu_t}{Sc_t} \frac{\partial Y_{\alpha}}{\partial x^i} \quad (18)$$

Diffusion Stress

It was found that the apparent diffusion stress term τ_D^{ji} arising from the mixture momentum equation was an essential part in our simulations and hence forth it has been included in our current work. Readers are advised that this term does not exist normally within the framework of ANSYS-CFX 10 and it has been explicitly added into the slip velocity and momentum equations. In this paper, no interactions between dispersed phases, other than the hindrance of settling phases similar to Fletcher and Brown (2009), have been taken into account.

Solution of the above equations by analytical techniques is not possible. ANSYS-CFX 10 uses a finite volume method to solve the above equations on an unstructured grid. Coupling between pressure and velocity in equations (1) and (2) is handled implicitly by the coupled solver and to avoid checker-board oscillations in the flow field variables the Rhie and Chow (1983) interpolation procedure is used. The second order accurate "High Resolution Scheme" is used to discretise advection terms in the equations to improve solution accuracy. Scalable wall functions within ANSYS-CFX were used for the treatment at the walls. In all simulations the $y+$ values were typically 30. Further details of the solution procedure and turbulence model and their constants are given in Anon (2005).

FLOW CONDITIONS IN THE SETTLING TANK

The test case settling tank has a diameter of 20m. A flow of $1200 \text{ m}^3 \text{ h}^{-1}$ enters through a tangential inlet into a 4m diameter feedwell fitted with a shelf placed at a distance of 1.0 m from the top. 10% of the flow is considered to leave through the underflow, with the remainder through the overflow. To realise the same in CFD, a mass flow outlet is specified for the underflow, whereas a pressure outlet is specified at the overflow. The geometry of the test case settling tank is shown in Figure 1.

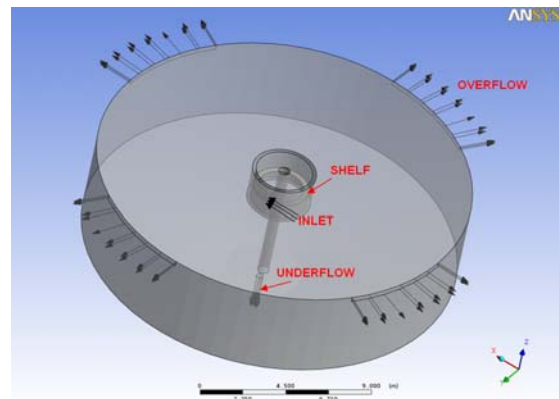


Figure 1: Schematic diagram of tank geometry.

The phases considered in this study were sand, clay (both settling phases) and a floatable phase. The dispersed phase properties are summarised in Table 1. Two size variants of

the floatables are used in our simulations to test their size dependency.

Table 1: Modelling conditions.

Phase	Density (kg m ⁻³)	Diameter
Floatables	980	3.0 mm (S1)
		1.0 mm (S2)
Clay	2500	100 µm
Sand	2500	200 µm

RESULTS

Figure 2 shows the turbulent kinetic energy (TKE) plot of the settling tank considered in this study. It can be seen from the plot that the turbulence is maximum in the feedwell region just aft of the inlet. This region of higher turbulence and shear rates has often been exploited through the addition of flocculant to aid effective and better flocculation of secondary phase particles. This in turn makes the suspended phase settle faster due to the increase in its bulk density. Flocculation and its effect on the flow pattern have not been considered in this study.

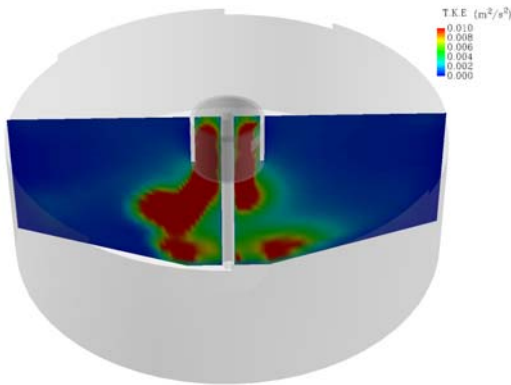


Figure 2: Turbulent Kinetic Energy (TKE) contour.

At the feedwell exit, the TKE is still high opposite the inlet, as the bulk of the flow is discharged out through this region. Due to the tangential inlet into the feedwell, an asymmetric pattern of TKE is well pronounced.

Floating Solids Results

Figure 3a and 3b shows the predicted volume fraction of the floating phase along selected horizontal planes of the test case feedwell for floatable diameters of 3.0 and 1.0 mm, respectively. In each case the lowest represents the exit plane, just below the base of the feedwell.

With the current volumetric throughput assumption, the test case feedwell is considered to be well mixed. The only major significant difference between the dimensions of the dispersed phase is noted in the exit plane, with some preferential discharge of the floating phase to one side for a diameter of 3.0 mm. There is a tendency for larger particles to move independently of the fluid flow as they exhibit a larger slip velocity as well as a larger Stokes number. The Stokes number here is defined as the ratio of the particle relaxation time (t_p) to a time characteristic of the fluid motion (t_s), i.e. $St = t_p/t_s$. This determines the kinetic equilibrium of the particles with the surrounding liquid. In choosing the appropriate fluid time-scale t_s , the width (W_i) of the tangential inlet is taken as

the length-scale. The resulting time-scale is given by $t_s = W_i/U_o$ (here U_o is the feedwell inlet velocity). The major implication of the Stokes number is that particles with a small Stokes number ($St \ll 1$) are found to be in near velocity equilibrium with the surrounding carrier fluid, making them extremely or totally responsive to fluid velocity fluctuations. In fact they act as tracer particles used commonly in many non-intrusive measurement techniques (LDV/PIV/LDA). However, for a larger Stokes number ($St \gg 1$) particles they are no longer in equilibrium with the surrounding fluid phase, as they are unresponsive to fluid velocity fluctuations and they will pass unaffected through eddies and other flow structures, with a possibility to modify them. Based on the above definition, the Stokes number considered in our study are 1.25 and 0.14 for the 3.0 and 1.0 mm diameter floating phase, respectively. This also validates the use of the ASM model with assumption (i) above being valid for low Stokes numbers.

The distribution of particles in the downward moving flow at the exit plane of the feedwell is greater for 1.0 mm diameter particles (smaller Stokes number) than 3mm, and it could be expected that for an even smaller particle size the exit plane would have a uniform distribution of the dispersed floating phase. The larger the Stokes number for any dispersed phase, the greater is their tendency to behave independent of the carrier phase.

In extension to the above, Figure 4a represents the predicted fractions of the floating phase plotted on a vertical cross-section of the test tank for simulation S1. It can be seen that the phase collects at the top of the tank due to buoyancy. This layer thins just outside the feedwell and becomes thicker as one progresses towards the outer wall of the tank, with the maximum occurring at 1/3 the diameter from the centre of the tank. It again starts tapering away, as the floating phase is extracted out along with the water from the overflow. For both simulations S1 and S2, the asymmetric discharge from the feedwell into the tank is quite evident.

In comparison to Figure 4a, 4b shows a thicker band of this floating phase. With the smaller size, the layer of phase formed on the liquor surface within the main body of the tank penetrates significantly deeper. This is attributed to the fact that the diameter of the floating phase considered here is 1.0 mm, wherein they exhibit a lower Stokes number and hence disperse due to turbulence more easily in comparison to the larger sized floating specimen.

The main aim of the comparison was to demonstrate that the flow pattern as well the distribution of the floating phase would be dependent on the diameter of the floating particles. This may also have a tendency to impact the quality of the clarification zone near the top of the tank.

Settling Solids Results

In this section the simulated results of the settling solids (clay and sand) are presented. Figures 5 and 6 show the predicted volume fraction of the clay and sand respectively on selected vertical planes through the settling tank. While the feedwell is expected to be well mixed, there is evidence in all images of asymmetric discharge into the thickener. This is most apparent for the sand phase, as the size of this phase allows their passage to have independence from the feedwell continuous flow

patterns. In all likelihood the clay is discharged from the bottom of the feedwell symmetrically, with the asymmetry in the clay bed at the bottom of the thickener, being attributed to change in the flow field and the discharge pattern of sand (settling solid) along with the floatables from the feedwell.

Future work

A uniform temperature throughout the settling tank was assumed, while in reality there will be significant thermal gradients, particularly in colder months and when subjected to diurnal and nocturnal cycle. This is known to impact on flow patterns within the clarification zone, and has previously been captured in CFD modelling of a clarifier, with full-scale validation (Johnston et al., 1998). Our future studies are aimed in capturing these daily and seasonal temperature differences.

The predictions suggest that a benefit could be derived from ensuring the size of the floating phase during its passage through the tank is maintained or increased, i.e. that the turbulence encountered should be minimised or rather better controlled such that only that required for effective flocculation is applied. Although the diameters of floating phase considered in our current study are rather arbitrary, one could extend the model to include the effect of flocculation (Heath and Koh, 2003) on the size distribution of particles allowing for the optimisation of removal systems for such floatables.

CONCLUSION

CFD modelling of a floating phase was carried out in a test case settling tank. Along with the floating phase, two other solids with higher density that settle were also considered. Two size variants of the floating phase were modelled, one above a Stokes number of unity and the other below it. Inclusion of the diffusion stress term in the momentum equation was necessary to simulate both the floating and settling solids simultaneously. Accurate sizing of the floating phase could help in optimising the effective removal of the phase from the settling tank overflow.

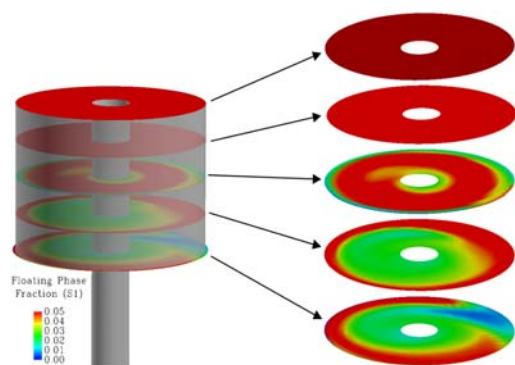


Figure 3a: Solids fraction of floating phase in the feedwell (S1)

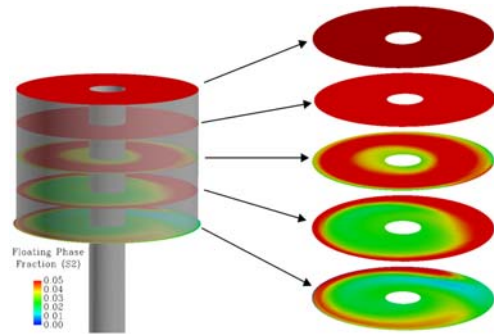


Figure 3b: Solids fraction of floating phase in the feedwell (S2)

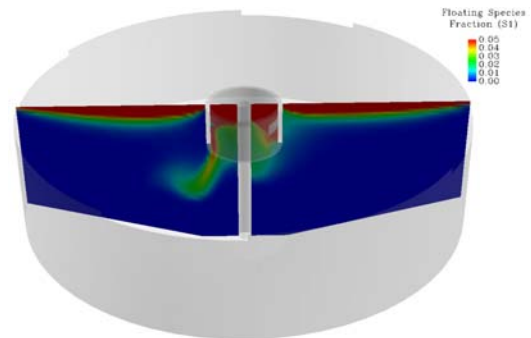


Figure 4a: Fraction of floating phase in a vertical cross-section of the settling tank (S1)

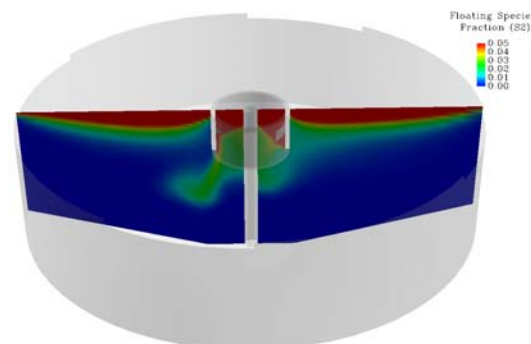


Figure 4b: Fraction of floating phase in a vertical cross-section of the settling tank (S2)

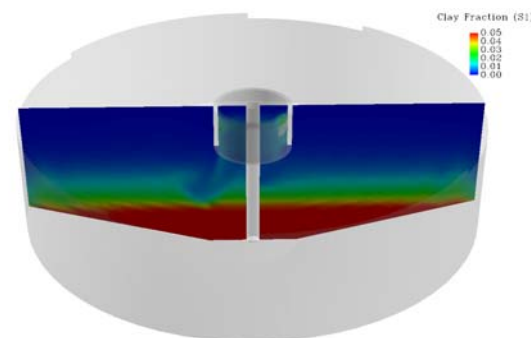


Figure 5a: Solids fraction of clay in a vertical cross-section of the settling tank (S1)

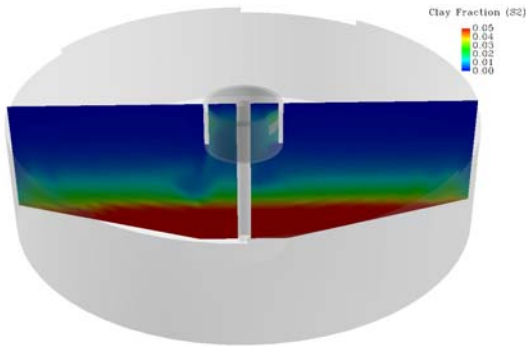


Figure 5b: Solids fraction of clay in a vertical cross-section of the settling tank (S2)

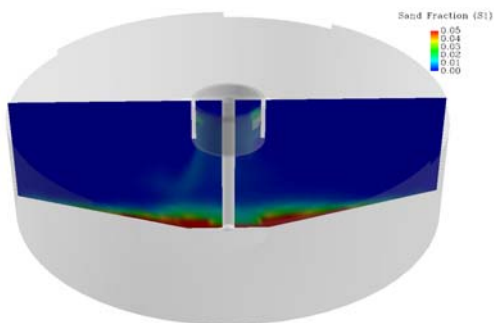


Figure 6a: Solids fraction of sand in a vertical cross-section of the settling tank (S2)

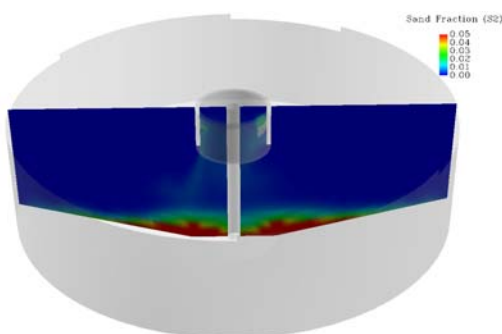


Figure 6b: Solids fraction of sand in a vertical cross-section of the settling tank (S2)

ACKNOWLEDGEMENTS

The support of the Parker CRC for Integrated Hydrometallurgy Solutions (established and supported under the Australian Government's Cooperative Research Centres Program) is gratefully acknowledged.

REFERENCES

- ADAMS, E.W. and RODI, W. (1990). "Modelling flow and mixing in sedimentation tanks", *Journal of Hydraulic Engineering*, **116**, 895–913.
- ADAMSSON, A., STOVIN, V. and BERGDAHL, L. (2003). "Bed shear stress boundary condition for storage tank sedimentation", *Journal of Environmental Engineering*, **129**, 651–658.
- ANDERSON, N.E. (1945). "Design of final settling tanks for activated sludge", *Sewage Works Journal*, **17**, 50–65.

ANON (2005). "ANSYS CFX Release 10.0 Documentation", *ANSYS Inc.*, Canonsburg USA, website address www.ansys.com/cfx.

BRETSCHER, U., KREBS, P. and HAGER, W.H. (1992). "Improvement of flow in final settling tanks", *Journal of Environmental Engineering*, **118**, 307–321.

BRENNAN, D. (2001). "The numerical simulation of two-phase flows in settling tanks", *PhD dissertation*, Imperial College of Science, Technology and Medicine, London.

CELIK, I., RODI, W. and STAMOU, A. (1985). "Prediction of hydrodynamic characteristics of rectangular settling tanks", *Proc. Int. Symp. Refined flow Modelling and Turbulence Measurements*, Iowa City, Iowa, USA.

DAHL, C.P., LARSEN, T. and PETERSEN, O. (1994). "Numerical modelling and measurement in a test secondary settling tank", *Water Science and Technology*, **30**, 219–228.

DUFRESNE, M., VAZQUEZ, J., TERFOUS, A., GHENAIM, A. and POULET, J.B. (2009). "Experimental investigation and CFD modelling of flow, sedimentation, and solids separation in a combined sewer detention tank", *Computers and Fluids*, **38**, 1042–1049.

ETCHELLS, A. (2001). "Mixing of floating solids", *Plenary conference ISMIP4*, 14–16 May 2001, Toulouse, France.

FAN, L., Xu, N., Ke, X. and Shi, H. (2007). "Numerical Simulation of Secondary sedimentation tank for urban wastewater", *Journal of Chinese Institute of Chemical Engineers*, **38**, 425–433.

FROST, R.C., HALLIDAY, J. and DEE, A.S. (1993). "Continuous consolidation of sludge in large scale gravity thickeners", *Water Science and Technology*, **28**, 77–86.

FULFORD, J.M. (1995). "Effects of pulsating flow on current meter performance". In *Proceedings 1st International Conference on Water Resources Engineering, ASCE*.

FLETCHER, D.F. and BROWN, G.J. (2009). "Numerical simulation of solids suspension via mechanical agitation: effect of the modelling approach, turbulence model and hindered settling law", *International Journal of Computational Fluids Dynamics*, **23**, 173–187.

HEATH, A.R. AND KOH, P.T.L. (2003). "Combined Population Balance and CFD Modelling of Particle Aggregation by Polymeric Flocculant", *3rd International Conference on CFD in the Mineral and Process Industries, CSIRO*, Melbourne, Australia, 10–12 December.

IMAM, E., McCORQUODALE, J.A. and BEWTRA, J.K. (1983). "Numerical modelling of sedimentation tanks", *Journal of Hydraulic Engineering*, **109**, 1740–1754.

JAYANTI, S. and NARAYANAN, S. (2004). "Computational study of particle-eddy interaction in sedimentation tanks", *Journal of Environmental Engineering*, **130**, 37–49.

JOHNSTON, R. R. M, SCHWARTZ, P., NEWMAN, M., KERSHAW, M., SIMIC, K., FARROW, J. B., SWIFT, J. D. (1996). "Improving thickener performance at Pasminco Hobart Smelter," *Zinc and Lead Processing*, Dutrizac, JE, Gonzalez, JA, Bolton, GL and Hancock, P (Eds), Canad. Inst. Mining, Metall. Petrol., 697–713.

KAHANE, R., NGUYEN, T. V. and SCHWARZ, M. P. (2002). "CFD modelling of thickeners at Worsley Alumina Pty Ltd", *Appl. Math. Modelling*, **26**, 281–296.

- KREBS, P., ARMBRUSTER, M. and RODI, W. (1998). "Laboratory experiments of buoyancy-influenced flow in clarifiers." *Journal of Hydraulic Research*, **36**, 831–851.
- KHAZAM, O. and KRESTA, S.M. (2009). "Drawdown of floating solids in stirred tanks", *13th European Conference on Mixing*, London, 14-17 April 2009.
- KUZMANIC, N. and RUSIC, D. (1999). "Solids concentration measurements of floating particles suspended in a stirred vessel using sample withdrawal techniques", *Ind. Chem. Eng. Res.* **38**, 2794–2802.
- LAKEHAL, D., KREBS, P., KRIJGMAN, J. and RODI, W. (1999). "Computing shear flow and sludge blanket in secondary clarifiers". *Journal of Hydraulic Engineering*, **125**, 253–262.
- LARSEN, P. (1977). "On the hydraulics of rectangular settling basins", *Report No.1001*, Department of Water Resource Engineering, Lund Institute of Technology, Lund, Sweden.
- LYN, D.A. and RODI, W. (1990). "Turbulence measurements in model settling tank", *Journal of Hydraulic Engineering*, **116**, 3–21.
- LYN, D.A., STAMOU, A. and RODI, W. (1992). "Density currents and shear-induced flocculation in sedimentation tanks", *Journal of Hydraulic Engineering*, **118**, 849-867.
- MACKIEWICZ, B. and KARZCZ, J. (2009). "CFD modelling of suspension of floating particles", *Chemical and Process Engineering*, **30**, 111-123.
- MOORE, P. (2009). "The oil sands life cycle", *Mining Magazine*, May 2009, 28-33.
- NGUYEN, T., HEATH, A. and WITT, P. (2006). "Population balance-CFD modelling of fluid flow, solids distribution and flocculation in thickener feedwells", *5th International Conference on CFD in Process Industries*, CSIRO, 13th-15th December, Melbourne.
- RHIE, C.M. and CHOW, W.L. (1983). "Numerical study of the turbulent flow past an airfoil with trailing edge separation", *AIAA Journal*, **21**, 1527-1532.
- SCHILLER, L. and NAUMANN, A. (1933). *VDI Zeits*, **77**, p318.
- STAMOU, A., ADAMS, E.W. and RODI, W. (1989). "Numerical modelling of flow and settling in primary rectangular clarifiers", *IAHR*, **27**, 665–682.
- STAMOU, A. (1991). "On the prediction of flow and mixing in settling tanks using a curvature-modified k-ε model", *Appl. Math. Modelling*, **15**, 351–358.
- TAGAWA, A., DOHI, N. and WEI, H. (2006). "Dispersion of floating solid particles in aerated stirred tank reactors: minimum impeller speeds for off-surface and ultimately homogeneous solid suspension and solids concentration profiles", *Industrial and Engineering Chemistry Research*, **45**, 818-829.
- TASKIN, G.O. and WEI, H. (2003). "The effect of impeller-to-tank diameter ration on draw down solids", *Chemical Engineering Science*, **58**, 2011-2022.
- UEBERL, J. and HAGER, W.H. (1997). "Improved design of final settling tanks". *Journal of Environmental Engineering*, **123**, 259–268.
- VANROLLEGHEM, P.A., De CLERCQ, B., De CLERCQ, J., DEVISSCHER, M., KINNEAR, D.J. and NOPENS, I. (2006). "New measurement techniques for secondary settlers: A review". *Water Science and Technology*, **53**, 419-429.
- ZHOU, S. and MCCORQUODALE, J.A. (1992). "Modelling of rectangular settling tanks", *Journal of Hydraulic Engineering*, **118**, 1391-1405.